Optimal operation management of microgrids using the point estimate method and firefly algorithm while considering uncertainty

Sirus MOHAMMADI[1,*], **Babak MOZAFARI**[2], **Soodabeh SOLEYMANI**[2]
[1]Department of Electrical Engineering, Gachsaran Branch, Islamic Azad University, Gachsaran, Iran
[2]Department of Electrical Engineering, Science and Research Branch, Islamic Azad University, Tehran, Iran

Abstract: This paper analyzes the behavior of Hong's point estimate method to account for uncertainties in probabilistic energy management systems to optimize the operation of a microgrid (MG). These uncertainties may arise from different sources, such as the market prices, load demands, and electric power generation of wind farms and photovoltaic systems. Point estimate methods constitute a remarkable tool to handle stochastic power system problems because good results can be achieved using the same routines as those corresponding to deterministic problems, while keeping the computational burden low. The problem is formulated as a nonlinear constraint optimization problem to minimize the total operating cost. Weibull, beta, and normal distributions are used to model the uncertain input variables in this study. Moreover, the firefly algorithm is applied to achieve optimal operational planning with regard to cost minimization. The efficiency of Hong's point estimate method is validated on a typical MG. Results for the case study are presented and compared against those obtained from the Monte Carlo simulation. Specifically, this paper shows that the use of the $2m+1$ scheme provides the best performance when a high number of random variables, both continuous and discrete, are considered.

Key words: Probabilistic energy management, microgrid, point estimate methods, operation cost

1. Introduction

In recent years, there has been a global movement in the direction of the adoption and deployment of distributed and renewable resources. Renewable energy (RE) sources differ from conventional sources in that generally they cannot be scheduled, they are much smaller than conventional power stations, and they are often connected to an electricity distribution system rather than a transmission system. The integration of such time-variable distributed or embedded sources into electricity networks requires special consideration. Due to the ever-increasing demand for high-quality and reliable electric power, the concept of distributed energy resources (DERs) has attracted widespread attention in recent years [1]. DERs consist of relatively small-scale generation and energy storage devices that are interfaced with low- or medium-voltage distribution networks and can offset the local power consumption, or even export power to the upstream network if their generation surpasses the local consumption. A new philosophy of operation that is expected to enhance the utilization of DERs is known as the microgrid (MG) concept [2,3]. MGs should widely utilize RE resources such as wind, sunlight, and hydrogen to play a significant role in the electric power systems of the future, for cleaner air, reduced transmission and distribution costs, and the enablement of energy efficiency enhancement initiatives. In addition, using energy storage devices such as batteries, energy capacitors, flywheels, or controllable loads along with distributed generation (DG) units makes MGs operate in a more flexible and economic manner [4,5]. From a customer's

---

*Correspondence: s.mohammadi@iaug.ac.ir

point of view, MGs similar to traditional low-voltage (LV) distribution networks not only provide their thermal and electricity needs, but, in addition, enhance local reliability, reduce emissions, improve power quality by supporting voltage and reducing voltage dips, and lead to lower costs of the energy supply [6].

Several studies were performed to optimize the operation, load dispatch, and management of energy storage systems of MGs. The particle swarm optimization (PSO) method, accordingly, was employed in [7] to minimize the cost of MGs with controllable loads and battery storage. This was done by selling the stored energy at high prices and shaving peak loads of the larger system. A linear programming algorithm was used in [8] to optimize MG operation cost and battery charge states. Maximizing of benefits owing to energy pricing differences between on-peak and off-peak periods was obtained by electrical and thermal storage charge scheduling in [9]. The authors in [10] presented a simple approach for predicting wind speed by means of short-term prediction. The proposed hybrid algorithm used the Hellman equation and a neural network to predict Hellman coefficients and wind speed. The autoregressive moving average algorithm was then used for short-term wind speed and power prediction. Morais et al. [11] proposed the classical unit commitment. Dukpa et al. [12] proposed a new optimal participation strategy for a wind power generator that employs an energy storage device for participating in a day-ahead unit commitment process considering stochastic power output.

The important drawback of the above works is that they do not consider all of the uncertainties of the problem. Although employing RE sources obviates environmental concerns and fossil fuel consumption, it introduces uncertain and fluctuating power because of stochastic wind and solar variation [13]. In addition, regarding the open-access power market and diverse commercial, residential, and industrial consumer types, the daily load demand also has a random nature [14]. Moreover, in an open-access power market, the degree of uncertainty of the load forecast error and market price can be even more perceptible [14]. Engineers require computational methods that could provide solutions less sensitive to the environmental effects, so techniques should be used that take uncertainty into account to control and minimize the risks associated with design and operation [15]. In order to consider uncertainty in the optimal energy management planning of MGs effectively, the optimization problem should be solved for a suitable range of each uncertain input variable instead of just one estimated point. Using a deterministic optimization problem, a large computational burden is required to consider every possible and probable combination of uncertain input variables. Hence, from a system planning point of view, it turns out to be convenient to approach the problem of the energy management planning of MGs as a probabilistic problem. This leads to a problem known as energy management planning under uncertainty, where the output variable of a MG objective function is obtained as a random variable, and thus it becomes easy to identify the possible ranges of the total operating cost.

There are several techniques for dealing with problems under uncertainty. The 3 main approaches are analytical, simulation (Monte Carlo simulated), and approximate methods [16]. The vast majority of techniques have been analytically based and simulation techniques have taken a minor role in specialized applications. The main reason for this is that simulation generally requires large amounts of computing time, and analytical models and techniques have been sufficient to provide planners and designers with the results needed to make objective decisions [17]. Moreover, analytical models require some mathematical assumptions in order to simplify the problem.

Simulation methods estimate uncertainty by simulating the actual process and random behavior of the system. The techniques can theoretically take into account virtually all aspects and contingencies inherent in the planning, design, and operation of a power system [17]. The main drawback of the simulation (Monte Carlo) is the great number of simulations required to attain convergence.

Approximate methods give an approximate description of the statistical properties of output random variables. These methods provide a satisfactory balance between speed and precision. Among these techniques, the first-order second-moment [18] and point estimate methods stand out. The point estimate method [19] can be used to calculate the statistical moments of a random quantity that is a function of one or several random variables and has been used in the transfer capability uncertainty computation [20]. The focus in use of the point estimate method may be on simultaneously and efficiently evaluating several probability distributions of a system.

In this paper, the point estimate method is devised to optimize the energy management of MGs. The main advantages of point estimate methods are that they use deterministic routines for solving probabilistic problems and overcome the difficulties associated with the lack of perfect knowledge of the probability functions of stochastic variables, since these functions are approximated using only their first few statistical moments (i.e. mean, variance, skewness, and kurtosis).

The aim of any point estimate technique is to compute the moments of a random variable Z that is a function of m random input variables p_l, i.e. $Z = F(P_1, P2_{,...,} Pm)$. The first point estimate method was proposed by Rosenblueth in 1975 [21] for only symmetric variables, and it was later revisited in 1981 [22] to consider asymmetric variables. Since then, several methods that improve the original Rosenblueth method have been presented. They mainly differ in the type of random variables they consider (symmetric or asymmetric, correlated or not) and on the number of evaluations to be performed.

In practical power system problems, the number of input random variables involved is high [23]. Therefore, the original Rosenblueth method, as well as recent and more accurate point estimate methods based on the Rosenblueth approach [24,25], are not appropriate because the number of simulations could be even greater than in the Monte Carlo simulation. Moreover, the number of simulations to be performed using the point estimate methods developed by Harr [26] or Hong [27] grows linearly with the number of input random variables. Moreover, although Harr's method is appropriate for correlated variables, it is constrained to symmetric variables (skewness equals zero).

In this paper, Hong's point estimate schemes are devised to optimize the energy management of MGs to take into account the uncertainty in the MG's parameters. Three different concentration schemes are presented and tested over a typical MG. The results are compared against those obtained using a Monte Carlo simulation.

2. Operation management of a MG

2.1. Objective function

The objective function for each hour's intervals can be written as:

$$Minf(X) = \sum_{t=1}^{NT} Cost^t = \sum_{t=1}^{NT} \{ \sum_{i=1}^{N_g} [u_i^t p_{Gi}^t B_{Gi}^t + S_{Gi} |u_i^t - u_i^{t-1}|] $$
$$+ \sum_{j=1}^{N_s} [u_j^t p_{sj}^t B_{sj}^t + S_{sj} |u_j^t - u_j^{t-1}|] + p_{Grid}^t B_{Grid}^t \}, \tag{1}$$

where $\mathbf{X} = [X^1 X^2 ... X^t ... X^{NT}]$ and X^t is a state variable vector, including the active powers of the units and their related states, which can be described as follows:

$$X^t = [p_{G1}^t, p_{G2}^t, ..., p_{GNg}^t, p_{s1}^t, p_{s2}^t, ..., p_{sNs}^t, u_1^t, u_2^t, ..., u_{Ns+Ng}^t]. \tag{2}$$

2.2. Constraints

Unit constraints in energy management systems, including the unit capacity, ramping rates, minimum up/down, crew, fuel, start-up, shut-down, and AC power transmission constraints, calculate the commitment of the units for supplying the hourly load. The constraints for the problem are as follows.

2.2.1. System power balance

The total power generation from DGs in the MG must cover the total demand inside the grid. Hence,

$$\sum_{i=1}^{N_g} p_{Gi}^t + \sum_{j=1}^{Ns} p_{sj}^t + p_{Grid}^t = \sum_{D=1}^{N_D} P_{L_D}^t. \tag{3}$$

2.2.2. Unit generation output limits

For a steady state operation, the active power output of each DG is limited by the lower and upper bounds, as follows:

$$p_{Gi,\min}^t \leq p_{Gi}^t \leq p_{Gi,\max}^t, p_{sj,\min}^t \leq p_{sj}^t \leq p_{sj,\max}^t, p_{grid,\min}^t \leq p_{Grid}^t \leq p_{grid,\max}^t. \tag{4}$$

2.2.3. Spinning reserve constraint

$$\sum_{i=1}^{N_g} u_i^t p_{Gi,\max}^t + \sum_{j=1}^{Ns} u_j^t p_{sj,\max}^t + p_{grid,\max}^t \geq \sum_{D=1}^{N_D} P_{L_D}^t + R^t. \tag{5}$$

2.2.4. Charge and discharge rate limit related to the storage device

Due to the fact that there are some limitations on the discharge and charge rates of storage devices during each time interval, the following equation and constraint can be considered for a typical battery:

$$W_{ess}^t = W_{ess}^{t-1} + \eta_{ch\,arg\,e} P_{ch\,arg\,e} \Delta t - \frac{1}{\eta_{disch\,arg\,e}} P_{disch\,arg\,e} \Delta t, \tag{6}$$

$$\begin{cases} W_{ess,\min} \leq W_{ess}^t \leq W_{ess,\max} \\ P_{ch\,arg\,e,t} \leq P_{ch\,arg\,e,\max}; P_{disch\,arg\,e,t} \leq P_{disch\,arg\,e,\max} \end{cases}. \tag{7}$$

3. Hong's point estimate method

Point estimate methods can be used to calculate the statistical moments of a random quantity that is a function of one or several random variables and have been used in transfer capability uncertainty computations. These methods concentrate the statistical information provided by the first few central moments of a problem's input random variable on K points for each variable, named *concentrations*. Using these points and function F, which relates to the input and output variables, information about the uncertainty associated with the problem's output random variables can be obtained. The *Kth* concentration $(p_{l,k},\ w_{l,k})$ of a random variable p_l can be defined as a pair composed of a location $p_{l,k}$ and a weight $w_{l,k}$. The location $p_{l,k}$ is the *Kth* value of variable p_l, at which function F is evaluated. The weight $w_{l,k}$ is a weighting factor that accounts for the relative importance of this evaluation in the output random variables. Using Hong's method, function F has to be evaluated only K times for each input random variable p_l at the K points made up of the *Kth* location $p_{l,k}$ of the input random

variable p_l and the mean (μ) of the $m-1$ remaining input variables, i.e. at the K points. In other words, the deterministic problem has to be solved K times for each input random variable p_l, and the difference among these problems is the deterministic value $p_{l,k}$ assigned to p_l, while the remaining input random variables are fixed to their corresponding mean. The number K of evaluations to be carried out depends on the *scheme* used. Therefore, the total number of evaluations of F is $K \times m$.

Specific variants, or schemes, of Hong's point estimate method take into account one more evaluation of function F at the point made up of the m input random variables means $(\mu_{p1}, \mu_{p2}, ..., \mu_{pl}, ..., \mu_{pm})$. Therefore, for these schemes, the total number of evaluations of F is $K \times m + 1$.

Let p_l be a random variable with probability density function (PDF) f_{pl}; then the k concentrations $(p_{l,k}, w_{l,k})$ of the m input random variables are obtained from the statistical input data. The location $p_{l,k}$ to be determined is [27]:

$$p_{l,k} = \mu_{pl} + \xi_{l,k} + \sigma_{pl}, \tag{8}$$

where μ_{pl} and σ_{pl} (input data) are the mean and standard deviation of the input random variable f_{pl}, and $\xi_{l,k}$ is the standard location. Weight $w_{l,k}$ and standard location $\xi_{l,k}$ are obtained by solving the nonlinear system of equations [27].

$$\begin{cases} \sum_{k=1}^{K} w_{l,k} (\xi_{l,k})^j = \lambda_{l,j}, j = 1, ..., 2k - 1 \\ \sum_{k=1}^{K} w_{l,k}(\xi_{l,k}) = \frac{1}{m} \end{cases} \tag{9}$$

This system can be solved using the procedure developed by Miller and Rice [28]. In this system, $\lambda_{l,j}$ is the ratio of the jth moments about the mean of p_l to $(\sigma_k)^j$; that is:

$$\lambda_{l,j} = \frac{M_j(p_l)}{(\sigma_{pl})^j}, \tag{10}$$

where

$$M_j(p_l) = \int_{-\infty}^{\infty} (p_l - \mu_{pl})^j f_{pl} dp_l. \tag{11}$$

Note that $\lambda_{l,1} = 0, \lambda_{l,2} = 1$ and $\lambda_{l,3}, \lambda_{l4}$ are, respectively, the skewness and kurtosis of p_l.

Once all of the concentrations $(p_{l,k}, w_{l,k})$ are obtained, function F is evaluated at points $(\mu_{p1}, \mu_{p2}, ..., \mu_{l,k}, ..., \mu_{pm})$, yielding $Z(l, k)$, where Z is the vector of the output random variables. The jth moment of the output random variables can be obtained from the proposed method using weighting factor $w_{l.k}$ and $Z(l, k)$ values as follows:

$$E(Z^j) \cong \sum_{l=1}^{m} \sum_{k=1}^{K} w_{l,k} \times [Z_i(l,k)]^j = \sum_{l=1}^{m} \sum_{k=1}^{K} w_{l,k} \times [F_i(\mu_{p1}, ..., p_{l,k}, ..., \mu_{pm})]^j. \tag{12}$$

The standard deviation of Z is computed as follows:

$$\sigma_Z = \sqrt{var(z)} = \sqrt{E(Z^2) - [E(Z)]^2}. \tag{13}$$

Three different concentration schemes ($2m$, $2m+1$, and $4m+1$) are considered in this paper. The $3m+1$ scheme is not considered since normally distributed input random variables yield complex standard locations and, thus, the concentration parameters are also useless nonreal values.

Analytically solving Eq. (9) to calculate the weights and standard locations is only possible for the $2m$ and $2m+1$ schemes. For $3m$ and $4m+1$, the solution of the system [Eq. (9)] can be obtained using Miller and Rice's procedure [28]. These 4 schemes are described below.

3.1. $2m$ scheme ($K = 2$)

If $K = 2$, the solution of the system of equations is given by:

$$\xi_{l,k} = \lambda_{l,3}/2 + (-1)^{3-k}\sqrt{m + (\lambda_{l,3}/2)^2}, k = 1, 2. \tag{14}$$

$\xi_{l,1}$ and $\xi_{l,2}$ depend on the m number of input random variables. While m increases, locations p_{l1} and p_{l2} move away from the mean μ_{pl} according to $\sqrt{m}$. The $\lambda_{l,3}$ expressed in Eq. (14) to denote the coefficient of skewness of p_l can be computed as follows:

$$\lambda_{l,3} = \frac{E[(p_l - \mu_{p_l})^3]}{(\sigma_{pl})^3}. \tag{15}$$

$w_{l,k}$, expressed in Eq. (16) to denote the weighting of the concentration located at $(\mu_{p1}, \mu_{p2}, ..., \mu_{l,k}, ..., \mu_{pm})$, is then used to scale these estimates to take into account the skewness of the probability distribution of Z.

$$w_{l,1} = -\frac{1}{m} \times \frac{\xi_{l,2}}{\xi_{l,1} - \xi_{l,2}}, \quad w_{l,2} = \frac{1}{m} \times \frac{\xi_{l,1}}{\xi_{l,1} - \xi_{l,2}} \tag{16}$$

The value of each $w_{l,k}$ ranges from 0 to 1 and the sum of all of the $w_{l,k}$ values is unity. The $2m$ scheme has important advantages related to its simplicity, its low computational burden, and the fact that it provides real-value solutions for the concentrations.

3.2. $2m + 1$ scheme ($K = 3$ and $\xi_{l,3} = 0$)

If 3 concentrations ($K = 3$) are used for each random variable and 1 of the locations of the concentrations is fixed at its mean value, we can match only the first 4 moments of the marginal PDF of the random variables. The solution of the system is:

$$\xi_{l,k} = \frac{\lambda_{l,3}}{2} + (-1)^{3-k}\sqrt{\lambda_{l,4} - \frac{3}{4}\lambda_{l,3}^2}, k = 1, 2 \text{ and } \xi_{l,3} = 0. \tag{17}$$

It can be seen that the standard location values of the $2m+1$ ($K \times m+1$) scheme do not depend on the number m of input random variables, as do the $K \times m$-type schemes.

The weights are:

$$w_{l,k} = \frac{(-1)^{3-k}}{\xi_{l,k}(\xi_{l,1} - \xi_{l,2})}k = 1, 2 \text{ and } w_{l,3} = \frac{1}{m} - \frac{1}{\lambda_{l,4} - \lambda_{l,3}^2}. \tag{18}$$

By noting that m of $3m$ concentrations are located in the same point $(\mu_{p1}, \mu_{p2}, ..., \mu_{l,k}, ..., \mu_{pm})$ as the sum of the weights equal to w_0:

$$w_0 = \sum_{l=1}^{m} w_{l,3} = 1 - \sum_{l=1}^{m} \frac{1}{\lambda_{l,4} - \lambda_{l,3}^2}. \tag{19}$$

This $3m$ concentration scheme can be viewed as a $2m+1$ concentration scheme. From Eq. (17), we indicate that the $3m$ scheme yields nonreal locations because in the Weibull distribution $\lambda_{l,4} - (3/4) \times \lambda_{l,3}^2 < 0$.

The $2m+1$ scheme is more accurate than the $2m$ scheme because it takes into account the kurtosis $\lambda_{l,4}$ of the input random variables, while only 1 additional evaluation of function F is needed.

3.3. $3m$ scheme ($K = 3$)

For $K = 3$, the solution of the system [Eq. (9)] can be obtained using Miller and Rice's procedure, and the standard locations $\xi_{l,k}$ are the roots of this third-order polynomial:

$$\pi(\xi) = \xi^3 + C_2\xi^2 + C_1\xi + C_0, \tag{20}$$

where C_0, C_1, and C_2 are computed through:

$$\begin{bmatrix} \frac{1}{m} & 0 & 1 \\ 0 & 1 & \lambda_{l,3} \\ 1 & \lambda_{l,3} & \lambda_{l,4} \end{bmatrix} \times \begin{bmatrix} C_0 \\ C_1 \\ C_2 \end{bmatrix} = - \begin{bmatrix} \lambda_{l,3} \\ \lambda_{l,4} \\ \lambda_{l,5} \end{bmatrix}, \tag{21}$$

and then the concentration weights are given by:

$$w_{l,k} = \frac{1 + \frac{1}{m} \prod_{j \neq k} \xi_{l,j}}{\prod_{j \neq k} (\xi_{l,j} - \xi_{l,k})}. \tag{22}$$

The $3m$ scheme theoretically provides higher accuracy than the $2m$ scheme because it takes into account more detailed statistical information (the fourth and fifth central moments are also considered) of the random variable, and 3 points for each input random variable, instead of only 2, are considered. The $3m$ scheme usually provides useless complex concentration values when the Weibull distribution is used to model the input data uncertainty. If the input data uncertainty is modeled to normally distributed random variables, the $3m$ scheme becomes a $2m+1$ scheme. Therefore, this scheme is not used in this paper because we use the Weibull distribution for the wind power.

3.4. $4m + 1$ scheme ($K = 5$ and $\xi_{l,5} = 0$)

The $4m+1$ scheme is derived from the $5m$ scheme by setting to zero 1 of the 5 standard locations (let $\xi_{l,5} = 0$). Such as in the $3m$ scheme, there is not an analytical formula to calculate the concentration values. The other 4 standard locations $\xi_{l,k}$ are the roots of the following fourth-order polynomial:

$$\pi(\xi) = \xi^4 + C_3\xi^3 + C_2\xi^2 + C_1\xi + C_0, \tag{23}$$

where, C_0, C_1, C_2, and C_3 are computed through:

$$
\begin{bmatrix}
0 & 1 & \lambda_{l,3} & \lambda_{l,4} \\
1 & \lambda_{l,3} & \lambda_{l,4} & \lambda_{l,5} \\
\lambda_{l,3} & \lambda_{l,4} & \lambda_{l,5} & \lambda_{l,6} \\
\lambda_{l,4} & \lambda_{l,5} & \lambda_{l,6} & \lambda_{l,7}
\end{bmatrix}
\times
\begin{bmatrix}
C_0 \\
C_1 \\
C_2 \\
C_3
\end{bmatrix}
= -
\begin{bmatrix}
\lambda_{l,5} \\
\lambda_{l,6} \\
\lambda_{l,7} \\
\lambda_{l,8}
\end{bmatrix}.
\tag{24}
$$

Once $\xi_{l,1}, \xi_{l,2}, \xi_{l,3}$, and $\xi_{l,4}$ are obtained, the weights are determined by solving the linear system.

$$
\begin{bmatrix}
\xi_{l,1} & \xi_{l,2} & \xi_{l,3} & \xi_{l,4} \\
\xi_{l,1}^2 & \xi_{l,2}^2 & \xi_{l,3}^2 & \xi_{l,4}^2 \\
\xi_{l,1}^3 & \xi_{l,2}^3 & \xi_{l,3}^3 & \xi_{l,4}^3 \\
\xi_{l,1}^4 & \xi_{l,2}^4 & \xi_{l,3}^4 & \xi_{l,4}^4
\end{bmatrix}
\times
\begin{bmatrix}
w_{l,1} \\
w_{l,2} \\
w_{l,3} \\
w_{l,4}
\end{bmatrix}
=
\begin{bmatrix}
0 \\
1 \\
\lambda_{l,3} \\
\lambda_{l,4}
\end{bmatrix}
\tag{25}
$$

We take into account that the weight $w_{l,5}$ that corresponds to $\xi_{l,5} = 0$ is calculated by:

$$
w_{l,5} = \frac{1}{m} - \sum_{k=1}^{4} w_{l,k}.
\tag{26}
$$

In Eq. (8), setting $\xi_{l,5} = 0$ yields $p_{l,k} = \mu_{pl}$, and thus m of the $5m$ locations are the same $(\mu_{p1}, \mu_{p2}, ..., \mu_{l,k}, ..., \mu_{pm})$. Therefore, the weight of this concentration must be updated to the value w_0.

$$
w_0 = \sum_{l=1}^{m} w_{l,5} = 1 - \sum_{l=1}^{m} \sum_{k=1}^{4} w_{l,k}
\tag{27}
$$

For this reason, the $4m+1$ scheme can be viewed as a $5m$ scheme with a computational burden decrease of $m - 1$ evaluations of F.

4. Hong's point estimate method for computing the optimal production cost

The overall computational procedure of Hong's point estimate method is shown in Figure 1. The load demand, wind turbine (WT) power generation, photovoltaic (PV) power generation, and market price are some of the most uncertain variables in the new deregulated power systems, especially in MGs. For instance, the uncertainty of the load can stem from many different variables, like weather conditions, temperature variations, humidity, or programs pursued by governments. In the case of a WT, the wind speed variations as an input variable are converted to the output power, which can affect the total production. Similar discussions can be had for the PV production and market price.

Normal, beta, and Weibull distributions are used to handle the uncertain input random variables and, depending on the concentration scheme used, the locations and weights have to be computed as described previously. A deterministic analysis must be run for each point $(\mu_{p1}, \mu_{p2}, ..., \mu_{pl}, ..., \mu_{pm})$. Note that a deterministic routine may be used to carry out the computations because only deterministic values are involved. The cost function solution can be expressed as follows:

$$
Z(l, k) = F_i (\mu_{p1}, \mu_{p2}, ..., p_{l,k}, ...\mu_{pm}).
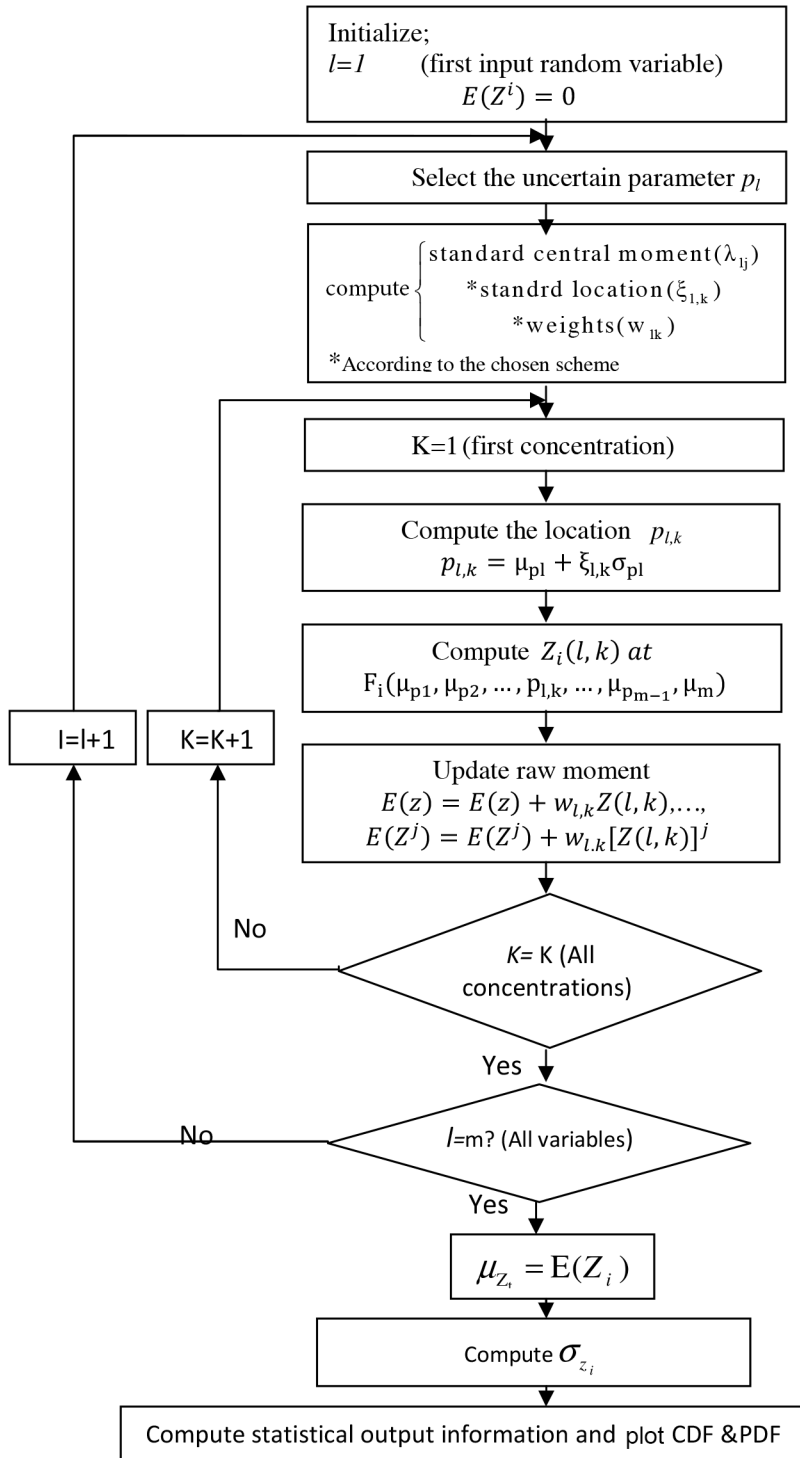\tag{28}
$$

Figure 1. Flow diagram of Hong's point estimate method.

Function f transfers the uncertainty from the input random variables to the output random variables and $Z(l, k)$ is the vector of the output random variables associated with the Kth concentration of random variable p_l. The total number of deterministic analyses to be run depends on the concentration scheme considered. The

vector of the output random variables is used to estimate the raw moments of the output random variables as follows:

$$
\begin{aligned}
E\left(Z\right) &\cong E(Z) + w_{l,k}Z(l,k) \\
E(Z^j) &\cong E(Z^j) + w_{l,k}(Z(l,k))^j
\end{aligned} \quad .
\tag{29}
$$

The process ends once all of the concentrations of all of the input random variables are taken into account. After that, the estimated raw moments of the output random variables are used to compute the desired statistical information. In order to obtain the PDFs and the cumulative density functions (CDFs) of the output random variables, the Gram–Charlier expansion is used [29]. To improve the optimization process, the firefly algorithm (FA) is utilized.

5. Firefly algorithm

The original FA was inspired by the behavior of firefly insects during the summer in tropical areas. The FA is a metaheuristic optimization algorithm that was first introduced at Cambridge University, based on 3 key ideas [30]: 1) given that any 2 fireflies may be attracted to each other, all fireflies are supposed to be unisex; 2) a firefly with less brightness is attracted to a firefly with more brightness and it is the brightness of each firefly that determines its attractiveness (light intensity); 3) in the case that no firefly with more brightness is recognized, a firefly can move randomly in the search space. It is worth noting that, in optimization problems, the brightness of a firefly is determined by the objective function value. The FA is a population-based optimization algorithm that has many similarities to other population-based algorithms, such as the artificial bee colony, PSO algorithm, and bacteria foraging optimization. However, the existence of some characteristics, like the low dependability of the algorithm on adjusting the parameters, the appropriate ability of a local search, and the simplicity of both idea and implementation, distinguish the FA from the rest. Moreover, the random characteristics of the FA allow the algorithm to perform a deep search for the global solution.

5.1. Distance between fireflies

The distance among the fireflies in the air is similar to the distance among the fireflies' vectors in the optimization search space. Consequently, any mathematical framework such as Cartesian (or Euclidean) distance, Mahalanobis distance, or Manhattan distance can be utilized to calculate the distance among the vectors of the fireflies. In this paper, the distance between the ith and jth fireflies is calculated in the Cartesian framework as follows:

$$
r_{ij} = \|X_i - X_j\| = \sqrt{\sum_{L=1}^{d} (x_{i,L} - x_{j,L})^2}.
\tag{30}
$$

5.2. Attractiveness of the fireflies

In reality, as the distance between 2 fireflies increases, less light can be seen by the fireflies (less attractiveness). In order to simulate this behavior of the fireflies, any monotonically decreasing function, as in Eq. (16), can be used [31]:

$$
\beta(r) = \beta_0 \times \exp(-\gamma r^m); m \geq 1.
\tag{31}
$$

5.3. Movement of the fireflies

One of the main ideas of the FA is that a firefly with less brightness is attracted to a firefly with more brightness. The movement of the jth firefly (with less brightness) toward the ith firefly (with more brightness) is mathematically formulated as follows:

$$X_j = X_j + \beta_0 \times \exp(-\gamma r^m) \times (X_i - X_j) + u_j$$
$$u_j = \alpha(rand - \tfrac{1}{2})$$
(32)

This equation consists of 3 segments: 1) the first segment is the current position of the jth firefly; 2) the second segment simulates the brightness of the ith firefly seen by the jth firefly; and 3) the third segment allows the jth firefly to move randomly in the entire search space when no brighter firefly is visible around it. The constant value α as the randomization parameter is in the range of (0,1).

However, there exist some points for the appropriate performance of the FA to be considered. According to recent works, it is shown that the tuning of the 2 variables, β_0 and γ, depends on the characteristics of the investigated problem. Consequently, there is no accurate formulation to give for the adjustment of these parameters for all types of optimization problems. Meanwhile, some keys should be regarded in all cases. As the distance between 2 fireflies is increased, the attractiveness of each firefly in view of the other firefly is reduced. Similarly, as the absorption coefficient γ reaches 0, the attractiveness coefficient (β) moves to β_0. Consequently, the distance between 2 fireflies does not have an effect on the light intensity, which simulates a local or global solution. This limiting feature corresponds to the original PSO algorithm [32]. In contrast, as the value of γ moves toward infinity, the bright density function is changed to a Dirac delta function ($\beta(r) \to \delta(r)$). This phenomenon simulates a situation in which the fireflies cannot see each other, so they have to move randomly.

6. Case study

A typical study case LV network, shown in Figure 2, was proposed in [27] and used in [6,28]. The system data were extracted from [6], where a complete data set can be found. The network comprises 3 feeders: 1 serving a primarily residential area, 1 industrial feeder serving a small workshop, and 1 feeder with commercial consumers. A variety of DG sources, such as microturbine (MT), proton-exchange membrane fuel cell, WT, PV, and nickel-metal-hydride battery, are installed in the network. It is assumed that all of the DG sources produce active power at a unity power factor, i.e. neither requesting nor producing reactive power. Moreover, the thermal load is not considered in the proposed MG system. Moreover, there is a power exchange link between the utility and the MG during the time step in the study period based on the decisions made by the MG central controller.

The maximum and minimum production limits of the DGs are given in Table 1. The bid coefficients in euro cents (€ ct) per kilowatt hour (kWh) are given in Table 2. Table 3 offers the real-time market energy prices for the examined period of time. In order to account for their production in the optimization functions, renewable source forecasting is required. A simple method that performs admirably well for very short-term forecasting and even outperforms most sophisticated state-of-the-art techniques in high temporal resolution applications is the 'persistence' method. This assumes that the renewable source production for the next time interval is equal to the current production and can be easily used in our application. The hourly forecasted load demand of the MG, the normalized forecasted output power of the WT and PV, and the hourly forecasted market price for a typical day can be found in Figure 3.
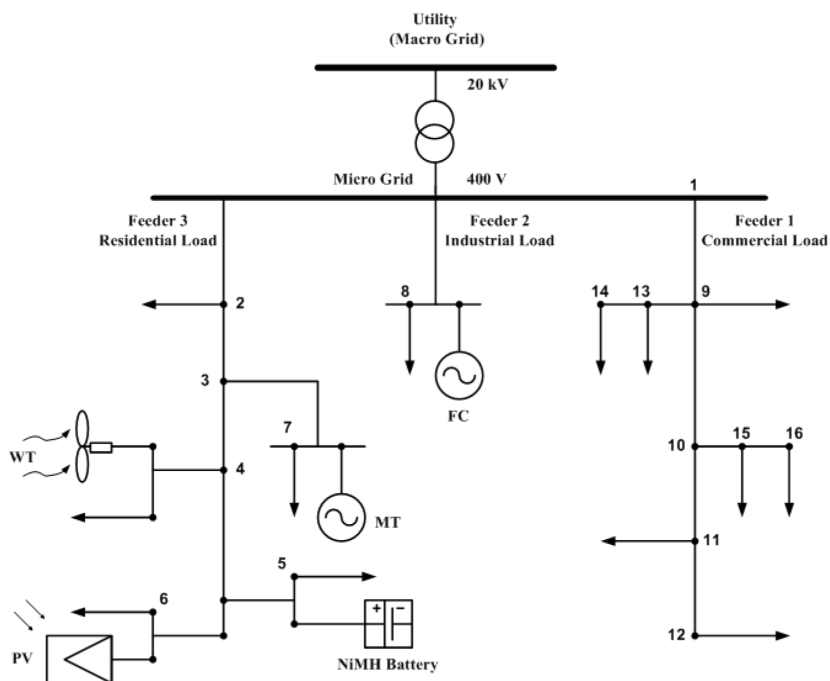
Figure 2. The study case LV network.

Table 1. The limits of the installed DG sources.

ID	Type	Min. power (kW)	Max. power (kW)
1	MT	6	30
2	PAFC	3	30
3	PV	0	25
4	WT	0	15
5	Bat	–30	30
6	Utility	–30	30

Table 2. Bids of the DG sources.

ID	Type	Bid (€ ct/kWh)	Start-up/shut-down cost (€ ct)
1	MT	0.457	0.96
2	PAFC	0.294	1.65
3	PV	2.584	0
4	WT	1.073	0
5	Bat	0.38	0

The total load demand within the MG for a typical day is 1695 kW. In this paper, the output power of the WT and the PV are considered equal to their forecasted values and the other value of the load demand is satisfied by the other units. In order to make the analysis simpler, it is assumed that the storages could supply or store power within their limit given in Table 1, without considering how much they were discharged or charged previously. Table 4 gives the detailed data of the economic dispatch and it can be inferred that all equality and inequity constraints are satisfied.

Table 3. Real-time market prices.

Price (€ ct/kWh)	Hour	Price (€ ct/kWh)	Hour
1.50	13	0.23	1
4.00	14	0.19	2
2.00	15	0.14	3
1.95	16	0.12	4
0.60	17	0.12	5
0.41	18	0.20	6
0.35	19	0.23	7
0.43	20	0.38	8
1.17	21	1.50	9
0.54	22	4.00	10
0.30	23	4.00	11
0.26	24	4.00	12
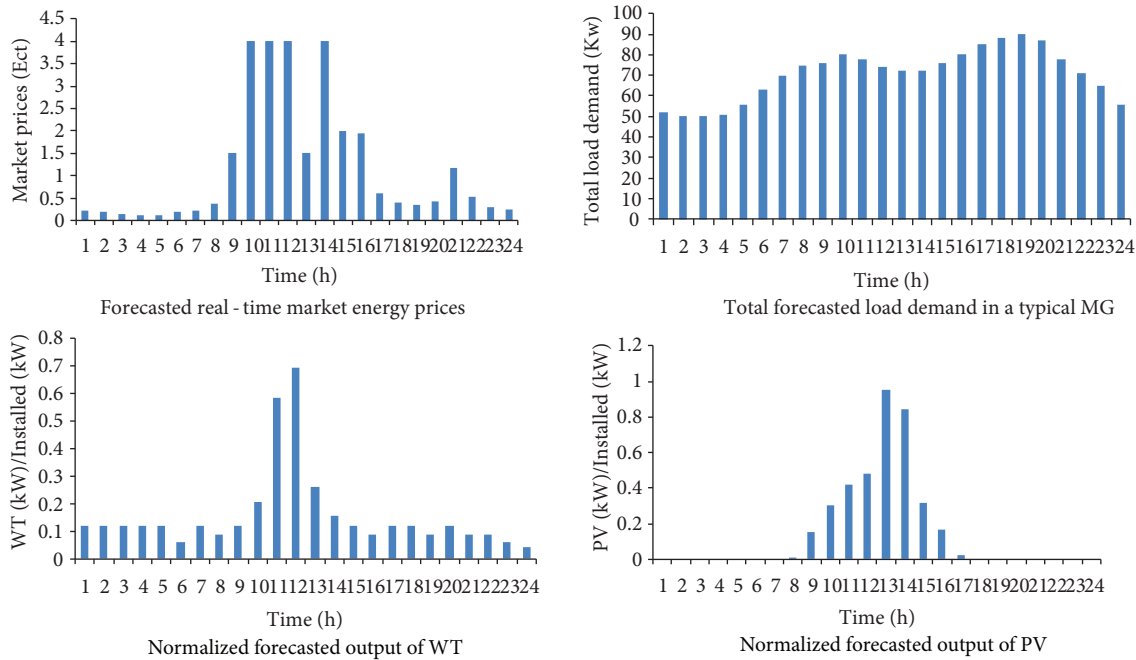
Figure 3. Forecasted values of the load demand, market price, and PV and WT power production.

The probabilistic data for the test system were obtained from [17,23,33,34]. The coefficient of variation, defined as the standard deviation and mean value ratio, is used to indicate the dispersion of the random variables [20]. The probabilistic data for the test system are determined as follows [12,21]:

- Load demand and market prices are modeled as normal distribution with a standard deviation of 5%.

- Output powers of the PV units have a beta distribution.

- The Weibull PDF is considered for the wind power.

In order to demonstrate the efficiency and accuracy of Hong's point estimate method, comparisons are made with the Monte Carlo simulation using 7000 samples. This amount of simulations is high enough to

guarantee the convergence of the Monte Carlo method. The differences among the solutions obtained by running several executions of the Monte Carlo simulation with 7000 samples are on the order of 10^{-4} per unit. These differences are small enough to consider the results provided by the Monte Carlo simulation with 7000 samples as reference or exact values.

Table 4. Economic dispatch.

Time (h)	MT (kWh)	PAFC (kWh)	PV (kWh)	WT (kWh)	Battery (kWh)	Utility (kWh)
1	6	29.43	0	1.7850	−13.4456	30
2	6	21.6326	0	1.7850	−14.7850	30
3	6	27.70	0	1.7850	−13.7855	30
4	6	21.80	0	1.7850	−12.7850	30
5	6	21.2433	0	1.7850	−11.7888	30
6	6.0004	29.12	0	0.8150	−3.9150	29.897
7	6.0004	21.3047	0	1.7850	12.2150	30
8	6	29.999	0	1.7855	20.8499	−15.6451
9	30	29.9999	0	1.7855	30	−20.5350
10	30	30	7.5250	3.0855	30	−20.6133
11	30	30	9.2277	8.7724	30	−30
12	30	30	11.9500	10.4133	30	−30
13	30	30	22.9000	3.91227	30	−27.77
14	30	30	16.0500	2.3785	30	−30
15	30	30	10.8450	1.7855	30	−15.6600
16	30	30	4.2250	1.3017	30	−11.4522
17	29.9999	30	0.5500	1.7854	30	−4.3542
18	6.0001	30	0	1.7855	30	24.1210
19	6	30	0	1.3021	29.6980	25
20	6.0007	329.99	0	1.7855	30	20.996
21	30	30	0	1.3010	30	−13.301
22	29.996	30	0	1.3010	30	−18.9484
23	6	29.96	0	0.9155	−12.9150	29.95
24	6	15.7852	0	0.6157	−10.6150	329.950

Table 5 shows the mean and standard deviation results of the total cast for the network, which have been considered as representative of the general results obtained from the different point estimate schemes analyzed in this paper. It is clear that the $2\ K \times m + 1$ type of schemes provide good results compared with the Monte Carlo values, both for the standard deviation and the mean. The $2m$ scheme results also yield acceptable values, but the differences are greater. This is due to the fact that the $2m$ scheme concentrations depend on the number m of input random variables. This effect was also mentioned in a previous work [35], applying point estimate methods to power systems. The $3m+1$ and $3m$ schemes were not considered due to the complex values obtained for the concentrations of the input random variables modeled with normal and Weibull distributions.

**Table 5.** Mean and standard diviation results for the total cost.

Parameters (μ, σ)	Methods			
	Monte Carlo	$2m$	$2m + 1$	$4m + 1$
Mean (μ)	274.3457	283.2336	274.3432	274.3447
Standard deviation (σ)	12.564	43.534	12.243	12.262

However, the $2m{+}1$ and $4m{+}1$ schemes maintain their good behavior when m increases because their concentrations do not depend on it. This stable behavior over the number of input random variables is the reason why these $K \times m{+}1$-type schemes provide better results than $K \times m$-type schemes when a practical power system is considered. Table 6 shows the error comparisons of different methods. The results for the test system (see Table 6) also show that the errors of the estimations incurred by schemes $2m{+}1$ and $m{+}1$ are much smaller than those corresponding to the estimations of the $2m$ scheme. For example, with regard to the mean values calculated by schemes $2m{+}$ 1 and $4m{+}1$, the largest error corresponding to the total cost does not exceed 0.0005%, but in the case of scheme $2m$, the highest error corresponds to the total cost, which is about 2.74%. As for the standard deviations, the differences between the estimations provided by the $2m$ scheme and those provided by the $Km + 1$ schemes are still more remarkable. For instance, the error associated with the estimation of the $2m$ scheme for the standard deviation of total cost is greater than 237%, whereas this error does not exceed 2.5% in the case of schemes $2m{+}1$ and $4m{+}1$.

Table 6. Error percentage in different methods.

Parameters (μ, σ)	Methods		
	$2m$	$2m + 1$	$4m + 1$
Mean	3.2%	0.00091%	0.0003%
Standard deviation	237.32%	2.55%	2.4%

Tables 5 and 6 show that Hong's point estimate method gives good modeling of the relationship between the cost function and the uncertain input parameters. In order to obtain the PDFs and the CDFs of the output random variables, the Gram–Charlier expansion is used. The PDFs of the operation cost are presented in Figure 4. In Figure 5, the CDFs are also compared with that obtained using Monte Carlo simulation. Figures 4 and 5 show that the PDF and CDF corresponding to the $2m{+}1$ scheme are almost not evident because they match those of the $4m{+}1$ scheme, and both provide good fitting to the CDF obtained with the Monte Carlo method. In Figure 5, the CDF estimated by the $2m$ scheme is different from the others.
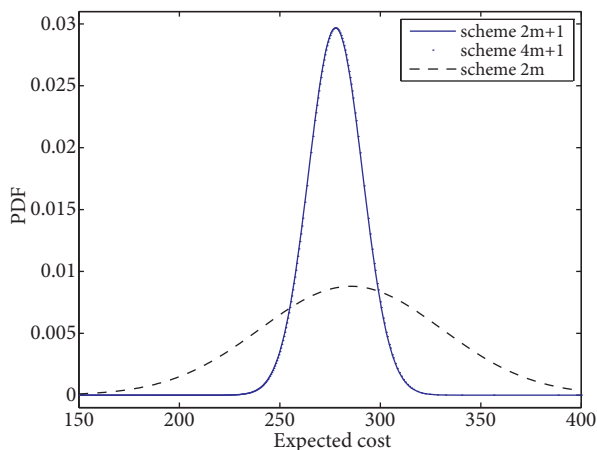
Figure 4. PDF of the expected cost.
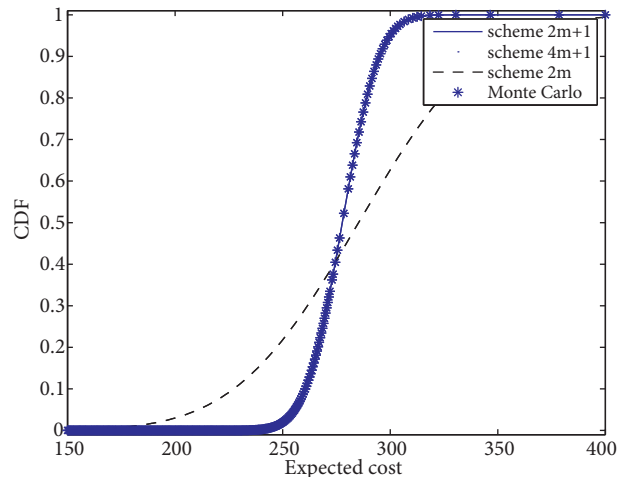
Figure 5. CDF of the expected cost.

This is another symptom of the bad behavior of the $2m$ scheme because there is a good fit for the mean but a high estimation error for the standard deviation. The $4m{+}1$ scheme exhibits the highest computational burden due to the high number of deterministic analysis performed.

On the other hand, it should be noted that the $2m+1$ scheme is faster than the $2m$ scheme, even though an additional deterministic cost function has to be solved. All of the simulations are carried out in MATLAB 7.12 on a Pentium-IV, core $i3$, 2.13-GHz personal computer with 3 GB of RAM. Table 7 shows the CPU time needed to analyze the statistical moments of the output variables for each scheme considered, as well as the Monte Carlo simulation with 7000 evaluations.

Table 7. CPU time (s).

	Methods			
	Monte Carlo	$2m$	$2m+1$	$4m+1$
CPU time	38.23	0.133	0.126	0.278

7. Conclusion

This paper presented a stochastic cost model to address the influence of the load demand, WT and PV unit generation, and market price uncertainties on the optimal operation of MGs.

The test results indicated that if the uncertain parameters considered can be measured or estimated, the distributions of all of the state variables and optimal costs can be accurately and efficiently evaluated with Hong's point estimate method.

The FA is a metaheuristic algorithm inspired by the flashing behavior of fireflies. The primary purpose for a firefly's flash is to act as a signal system to attract other fireflies. Since this problem is a type of nonlinear and complex optimization problem with equality and inequality constraints, a new optimization algorithm based on the adaptive modified FA (AMFA) is proposed. The proposed AMFA makes use of a powerful modification process to enhance the diversity of the firefly population, as well as a self-adaptive technique to increase the ability of the algorithm to move toward the promising global optimal solution quickly.

The $2m$, $2m+1$, and $4m+1$ schemes considered in this paper were tested on the stochastic cost model. Results were presented and compared against those obtained from the Monte Carlo simulation. Weibull and normal distributions were used to model input random variables. The results showed that the use of the $2m+1$ scheme provides the best performance. Similar results were obtained using the $4m+1$ scheme, although they implied a considerably higher computational burden. The $2m$ scheme accuracy decreases more than that of the other schemes because the $2m$ scheme concentrations depend on the number m of input random variables. Moreover, Hong's point estimate method was tested and verified by comparison with results from the Monte Carlo simulations on the test system. Using the results obtained from the Monte Carlo simulations as a basis, Hong's point estimate method could reach results similar to those of the Monte Carlo simulations with less effort in the numerical computations.

Nomenclature

p_l	Value of the lth input random variable
$p_{l,k}$	The kth location of p_l
$w_{l,k}$	The kth weighting factor of p_l
μ_{pl}	The mean of p_l
σ_{pl}	The standard deviation of p_l
$\xi_{l,k}$	The standard location of p_l
p_{Gi}^t, p_{sj}^t	Active power output of the ith generator and jth storage device at time t, respectively
p_{Grid}^t	Active power bought/sold from/to the utility at time t
B_{Gi}^t, B_{sj}^t	Bid of the jth DG source and jth storage device at hour t, respectively

B_{Grid}^t	Bid of the utility at hour t
S_{Gi}, S_{sj}	Start-up/shut-down costs for the ith DG unit and jth storage device, respectively
p_{LD}	The amount of the Dth load level
$p_{G,\min}^t, p_{G,\max}^t$	Minimum and maximum active power production of the ith DG at hour t, respectively
$p_{s,\min}^t, p_{s,\max}^t$	Minimum and maximum active power production of the jth storage at hour t, respectively
$p_{grid,\min}^t, p_{grid,\max}^t$	Minimum and maximum active power production of the utility at hour t, respectively
W_{ess}^t, W_{ess}^{t-1}	Battery energy storage at time t and $t-1$, respectively
$P_{Ch\,arg\,e}(P_{disch\,arg\,e})$	Permitted rate of charge (discharge) through a definite period of time Δt
$\eta_{ch\,arg\,e}(\eta_{disch\,arg\,e})$	Charge (discharge) efficiency of the battery
$W_{ess,\min}(W_{ess,\max})$	Lower and upper bounds on the battery energy storage, respectively
$P_{ch\,arg\,e,\max}(P_{disch\,arg\,e,\max})$	Maximum rate of charge (discharge) during a definite period of time Δt
R^t	The scheduled spinning reserve at time t
N	Total number of optimization variables
NT	Total number of hours
N_g	Total number of generation units
N_D	Total number of load levels
t, k	Time interval and iteration index, respectively
M	Number of input random variables of Hong's point estimate methods
u_i^t	Status of unit i at hour t
$\lambda_{l,3}$	The skewness of p_l
$\lambda_{l,4}$	The kurtosis of p_l
$E(z^j)$	The jth moment of the output random variable
N_s	Total number of storage units
$Z(l,k)$	The vector of the output random variables associated with the kth concentration of random variable p_l
d	The dimension of the control vector
γ	Absorption coefficient
r	Distance between any 2 fireflies
β_0	Initial attractiveness at r = 0

References

[1] V. Miranda, "Wind power, distributed generation: new challenges, new solutions", Turkish Journal of Electrical Engineering & Computer Sciences, Vol. 14, pp. 455–473, 2006.

[2] F. Katiraei, R. Iravani, N. Hatziargyriou, A. Dimeas, "Microgrids management", IEEE Power and Energy Magazine, Vol. 6, pp. 54–65, 2008.

[3] B. Kroposki, R. Lasseter, T. Ise, S. Morozumi, S. Papathanassiou, N. Hatziargyriou, "Making microgrids work", IEEE Power and Energy Magazine, Vol. 6, pp. 40–53, 2008.

[4] C. Chen, S. Duan, T. Cai, B. Liu, G. Hu, "Smart energy management system for optimal microgrid economic operation", IET Renewable Power Generation, Vol. 5, pp. 258–267, 2011.

[5] B. Dursun, C. Gökçöl, "Economic analysis of a wind-battery hybrid system: an application for a house in Gebze, Turkey, with moderate wind energy potential", Turkish Journal of Electrical Engineering & Computer Sciences, Vol. 20, pp. 319–333, 2012.

[6] A.G. Tsikalakis, N.D. Hatziargyriou, "Centralized control for optimizing microgrids operation', IEEE Transactions on Energy Conversion, Vol. 23, pp. 241–248, 2008.

[7] A.A. Moghaddam, A. Seifi, T. Niknam, M.R. Pahlavani, "Multi-objective operation management of a renewable MG (micro-grid) with back-up micro-turbine/fuel cell/battery hybrid power source", Energy, Vol. 36, pp. 6490–6507, 2011.

[8] S. Chakraborty, M.D. Weiss, M.G. Simoes, "Distributed intelligent energy management system for a single-phase high frequency AC microgrid", IEEE Transactions on Industrial Electronics, Vol. 54, pp. 97–109, 2007.

[9] C. Marnay, G. Venkataramanan, M. Stadler, A.S. Siddiqui, R. Firestone, B. Chandran, "Optimal technology selection and operation of commercial-building microgrids", IEEE Transactions on Power Systems, Vol. 23, pp. 975–982, 2008.

[10] O. Özgönenel, D.W.P. Thomas, "Short-term wind speed estimation based on weather data", Turkish Journal of Electrical Engineering & Computer Sciences, Vol. 20, pp. 335–346, 2012.

[11] H. Morais, P. Kàdàr, P. Faria, Z.A. Vale, H.M. Khodr, "Optimal scheduling of a renewable micro-grid in an isolated load area using mixed-integer linear programming", Renewable Energy, Vol. 35, pp. 151–156, 2010.

[12] A. Dukpa, I. Dugga, B. Venkatesh, L. Chang, "Optimal participation and risk mitigation of wind generators in an electricity market", IET Renewable Power Generation, Vol. 4, pp. 165–175, 2010.

[13] J. Hethey, S. Leweson, "Probabilistic analysis of reactive power control strategies for wind farms", MSc, Technical University of Denmark, 2008.

[14] A. Soroudi, M. Ehsan, R. Caire, N. Hadjsaid, "Possibilistic evaluation of distributed generations impacts on distribution networks", IEEE Transactions on Power Systems, Vol. 4, pp. 2293–2301, 2011.

[15] J.M. Morales, J. Perez-Ruiz, "Point estimate schemes to solve the probabilistic power flow", IEEE Transactions on Power Systems, Vol. 22, pp. 1594–1601, 2007.

[16] Y.K. Tung, B.C. Yen, Hydrosystems Engineering Uncertainty Analysis, New York, McGraw-Hill, 2005.

[17] R. Billinton, R. Allan, Reliability Evaluation of Power Systems, 2nd ed., New York, Plenum Press, 1996.

[18] M. Madrigal, K. Ponnambalam, V.H. Quintana, "Probabilistic optimal power flow", Proceedings of the IEEE Canadian Conference on Electrical and Computer Engineering, Vol. 1, pp. 385–388, 1998.

[19] E. Rosenblueth, "Point estimation for probability moments", Proceedings of the National Academy of Sciences of the USA, Vol. 72, pp. 3812–3814, 1975.

[20] C.L. Su, C.N. Lu, "Two-point estimate method for quantifying transfer capability uncertainty", IEEE Transactions on Power Systems, Vol. 20, pp. 573–579, 2005.

[21] E. Rosenblueth, "Two-point estimates in probability", Applied Mathematical Modelling, Vol. 5, pp. 329–335, 1981.

[22] K.S. Li, "Point-estimate method for calculating statistical moments", Journal of Engineering Mechanics - American Society of Civil Engineers, Vol. 118, pp. 1506–1511, 1992.

[23] A.L. Garcia, Probability, Statistics, and Random Processes for Electrical Engineering, Boston, Addison-Wesley Publishing Company, 1989.

[24] H.S. Seo, B.M. Kwak, "Efficient statistical tolerance analysis for general distributions using three-point information", International Journal of Production Research, Vol. 40, pp. 931–944, 2002.

[25] C.W. Tsai, S. Franceschini, "Evaluation of probabilistic point estimate methods in uncertainty analysis for environmental engineering applications", Journal of Environmental Engineering - American Society of Civil Engineers, Vol. 131, pp. 387–395, 2005.

[26] M.E. Harr, "Probabilistic estimates for multivariate analysis", Applied Mathematical Modelling, Vol. 13, pp. 313–318, 1989.

[27] H.P. Hong, "An efficient point estimate method for probabilistic analysis", Reliability Engineering & System Safety, Vol. 59, pp. 261–267, 1998.

[28] A.C. Miller, T.R. Rice, "Discrete approximations of probability distributions", Management Science, Vol. 29, pp. 352–362, 1983.

[29] P. Zhang, S.T. Lee, "Probabilistic load flow computation using the method of combined cumulants and Gram-Charlier expansion", IEEE Transactions on Power Systems, Vol. 19, pp. 676–682, 2004.

[30] X.S. Yang, Nature-Inspired Metaheuristic Algorithms, Frome, UK, Luniver Press, 2008.

[31] X.S. Yang, S.S. Hosseini, A.H. Gandomi, "Firefly algorithm for solving non-convex economic dispatch problems with valve loading effect", Journal of Soft Computing, Vol. 12, pp. 1180–1186, 2012.

[32] T. Apostolopoulos, A. Vlachos, "Application of the firefly algorithm for solving the economic emissions load dispatch problem", International Journal of Combinatorics, Article ID 523806, 2011.

[33] L.A. Sanabria, T.S. Dillon, "Power system reliability assessment suitable for a deregulated system via the method of cumulants", International Journal of Electrical Power & Energy Systems, Vol. 20, pp. 203–211, 1998.

[34] L. Freris, D. Infield, Renewable Energy in Power Systems, New York, Wiley, 2008.

[35] G. Verbic, C.A. Cañizares, "Probabilistic optimal power flow in electricity markets based on a two-point estimate method", IEEE Transactions on Power Systems, Vol. 21, pp. 1883–1893, 2006.